Light modulation at molecular frequencies

A. V. Sokolov, D. D. Yavuz, D. R. Walker, G. Y. Yin, and S. E. Harris

Edward L. Ginzton Laboratory, Stanford University, Stanford, California 94305

We describe the generation of amplitude- and frequency-modulated light with a modulation frequency equal to the fundamental vibrational frequency of molecular deuterium ($2994 \, \mathrm{cm}^{-1} \approx 90 \, \mathrm{THz}$). This is a first step toward the synthesis of subfemtosecond pulses with prescribed temporal shape.

It is well known that a carrier and two sidebands, depending on their relative phases, correspond to a frequency (FM) or amplitude modulated (AM) signal. Light is most often modulated by driving the dielectric constant of a material so as to produce phased sidebands with a frequency spacing of, at most, 150 GHz. In this Rapid Communication, we describe AM and FM light with a sideband spacing, and therefore modulation frequency, equal to the fundamental vibrational frequency of molecular deuterium ($2994 \, \mathrm{cm}^{-1} \approx 90 \, \mathrm{THz}$). We believe that this is a first step toward the synthesis of subfemtosecond pulses with prescribed temporal shape.

As a light source for this experiment, we use a recently developed collinear Raman generator [1,2]. This light source produces a comb of (at present) 17 sidebands spaced by about $2994 \, \mathrm{cm}^{-1}$ and extending from 2.94 μm in the infrared to 195 nm in the vacuum ultraviolet. The light source is based on the off-resonance adiabatic excitation of a Raman mode with a coherence that is sufficiently large that the importance of phase matching is negated and generation occurs collinearly. Although it was expected that sidebands obtained from such a source are mutually coherent, until now it was not clear if the relative phase among the sidebands remained the same across their temporal and spatial profiles. It is this uniform mutual coherence among the sidebands that allows the synthesis of AM and FM light, and in the future may lead to the generation of subfemtosecond pulses.

In this work we separate out and use only three sidebands (1.06 μm, 807 nm, and 650 nm) from the Raman comb. Frequency- or amplitude-modulated light is obtained by manually adjusting the relative phases of these sidebands. To detect this modulation, we make use of the fact that a Raman transition is driven by the near resonance component of the temporal envelope of the applied light intensity. These sidebands may be phased so that this component is either zero (FM), or maximized (AM). We note that it is essential that three sidebands be used in an experiment of this type. If two sidebands are used, as in coherent anti-Stokes Raman spectroscopy [3], then the magnitude of the envelope is independent of phase.

Our experimental setup is shown in Fig. 1. To construct the Raman generator, we use two transform-limited laser pulses at wavelengths of 1.0645 μm and 807.22 nm, such that the (tunable) laser-frequency difference is approximately equal to the fundamental vibrational frequency in D_2. The first laser is a Quanta-Ray GCR-290 Q-switched injection-seeded neodymium-doped yttrium aluminum garnet (Nd:YAG) laser, producing 100 mJ, 12 ns transform-limited pulses at a 10 Hz repetition rate. The second laser is a laboratory-built Ti:sapphire system, injection seeded from an external-cavity laser diode and pumped by the second harmonic of a separate Q-switched Nd:YAG laser. This laser produces 60 mJ, 18 ns pulses at the (tunable) seeding laser wavelength, which is monitored by a Burleigh WA-1500 Wavemeter (resolution of 50 MHz). The two driving laser pulses are synchronized by adjusting the delay between the two Nd:YAG laser Q-switch trigger pulses. The laser beams are combined on a dichroic beam splitter and are loosely focused to a nearly diffraction-limited spot in a D_2 cell. The 1.06 μm laser spot size is 460 μm, and the 807 nm laser spot size is 395 μm. The D_2 cell is cooled by liquid nitrogen to $T = 77$ K; the length of the cooled region is 48 cm. At a D_2 pressure of 50 to 100 torr and at a Raman detuning of a few hundred MHz, we observe collinear generation of a discrete spectrum with a bandwidth of about $50\,000 \, \mathrm{cm}^{-1}$ [1].

We use a prism to disperse the Raman sidebands and retain those with wavelengths 1.06 μm, 807 nm, and 650 mn. A partial reflector is used to attenuate the 1.06-μm beam, so that following the attenuation the ratio of the intensities of these beams are 1:14:1.2, respectively. The phase of the 650 nm beam is varied by tilting a glass plate (thickness 1.0 mm). The beams are then retroreflected and recombined into a new region of the D_2 cell (Fig. 1).
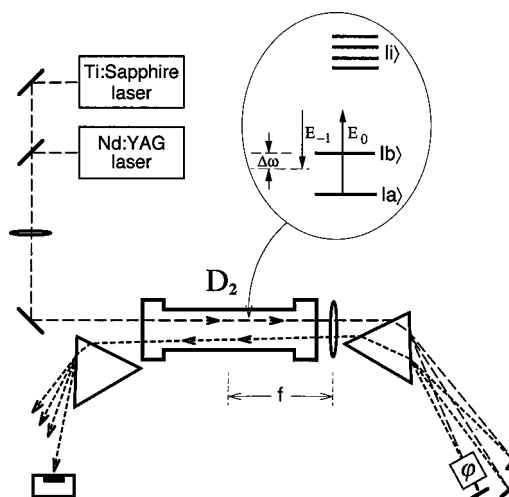

FIG. 1. Experimental setup and energy-level diagram for collinear Raman generation, synthesis of FM and AM light, and detection of the modulation.

This new region of the D_2 cell works as a detector for the AM component of the waveform. As the force on the nuclei is proportional to the electric field squared, and as the nuclei are too heavy to respond to the fast optical oscillations, the molecules respond to the variations in the intensity of light. The molecular motion, in turn, mixes with the 650-nm beam to generate the next anti-Stokes sideband at 544 nm. We measure the dependence of the intensity at 544 nm on the phase of the 650-nm beam.

In the ''detector'' region of the cell, the ensemble-averaged molecular oscillation is described by a normalized coordinate $\langle X \rangle = \rho_{ab} \cos(\omega_m t)$, where $\omega_m = 2994$ cm^{-1}. The magnitude $|\rho_{ab}|$ is proportional to the sum of the cross products of the adjacent field amplitudes [4]:

$$|\rho_{ab}|^2 \propto |E_0 E_{-1}^* + E_1 E_0^*|^2 \propto 1 + \frac{2|E_{-1}||E_1|}{|E_{-1}|^2 + |E_1|^2} \cos(\varphi), \quad (1)$$

where, following the notation of [4], E_{-1}, E_0, and E_1 are the (complex) field amplitudes of 1.06 μm, 807 nm, and 650 nm fields, respectively. The relative phase of the three sidebands is defined as $\varphi = \arg(E_1 E_0^*) - \arg(E_0 E_{-1}^*)$.

The two terms in Eq. (1), which drive the molecular oscillation, will interfere either constructively or destructively, depending on the relative phase of the sidebands. Figure 2 shows the interference fringes (at 26-torr D_2 pressure, Raman detuning $\Delta \omega = 800$ MHz), produced by measuring the peak intensity of the generated anti-Stokes field (at 544 nm) as a function of the relative phase φ of the three driving fields. In the small-signal limit, this intensity is proportional to the molecular coherence $|\rho_{ab}|^2$ [4]. Each data point is an average over ten laser shots, with error bars showing the standard deviation for each set. The experimental data are fitted by a theoretical curve produced with the assumption of perfect mutual coherence among the three sidebands and a constant ratio $|E_1/E_{-1}|$ [Eq. (1)]. The adjustable parameters in this fit are the vertical scaling and the initial phase φ_0. The ratio $|E_1/E_{-1}| = 1.1$ is measured experimentally, and the phase shift is calculated precisely from the parameters of the glass plate. The good quality of the fit represents the proof of the near-perfect mutual coherence among the three sidebands, across both their spatial and temporal profiles.

In the time domain, three sidebands spaced by 2994 cm^{-1} synthesize a periodic waveform with an 11.1-fs period (equal to the molecular oscillation period). When $\varphi = \pi$ (and $|E_1/E_{-1}| = 1$), the field intensity is constant, and the waveform is purely frequency-modulated (FM) and does not excite the molecular oscillation (this situation corresponds to the minima of Fig. 2). When $\varphi = 0$, the waveform is purely amplitude-modulated (AM) and efficiently drives the molecules at their resonant frequency (this situation corresponds to the maxima of Fig. 2).

From a different point of view, the plot of Fig. 2 can be considered as a time correlation of two beat notes: $(E_{-1} + E_0)$ and $(E_0 + E_1)$. A 2π shift in the relative phase φ corresponds to an 11.1-fs time delay between the beat notes. We use this relation to calculate the time delay from the relative phase in Fig. 2. The full width at half-maximum
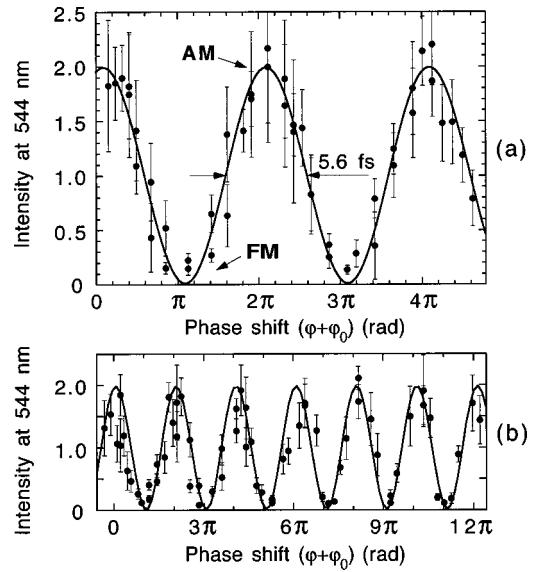

FIG. 2. Anti-Stokes generation at 544 nm (arbitrary units) as a function of the relative phase φ of the three sidebands (at 1.06 μm, 807 nm, and 650 nm). (a) Data set 1. (b) Data set 2, showing that additional phase retardation does not reduce the contrast. The solid line is produced from Eq. (1) by adjusting the vertical scaling and the experimentally unknown initial relative phase of the sidebands φ_0.

(FWHM) of a single peak in Fig. 2 corresponds to exactly half of the molecular period, 5.6 fs. It should be noted that if we use filters to make the intensities of the three sidebands equal, and adjust $\varphi = 0$, we will produce periodic pulses with a FWHM duration of (11.1 fs)/3 = 3.7 fs.

We now use the techniques of this work to further characterize the collinear Raman generator. In particular, we show that the phase of the molecular coherence, and therefore of the generated sidebands, changes by π when the difference of the two input frequencies is tuned from below to above the molecular resonance. This measurement is made as follows: Working at a D_2 pressure of 20 torr, we step through a sequence of Raman detunings and, at each detuning, tilt the glass plate so as to obtain a minimum in the fringe pattern. At each point the tilt angle is converted into the phase retardation at 650 nm. We find that mechanical shifts of the retroreflecting mirrors cause a slow phase drift of about one radian per ten minutes. We therefore intermittently measure the tilt angle, which is necessary to cause a minimum at a Raman detuning of 800 MHz and subtract this drift from the data.

Figure 3(a) shows the relative shift of the fringe pattern as a function of the Raman detuning. We observe a linear dispersion slope, caused by the difference in the beam path length for the three sidebands [in our setup the path for the 807-nm beam is 9.8 cm longer, and this delay is calculated to produce the dispersion of −4.1 rad/GHz in Fig. 3(a)]. In addition, we observe a distinct π-radian change in this shift, when tuning from one side of the Raman resonance to the other. This phase change corresponds to the transition from phased (driven below natural resonance) to antiphased (driven above natural resonance) molecular eigenstate.
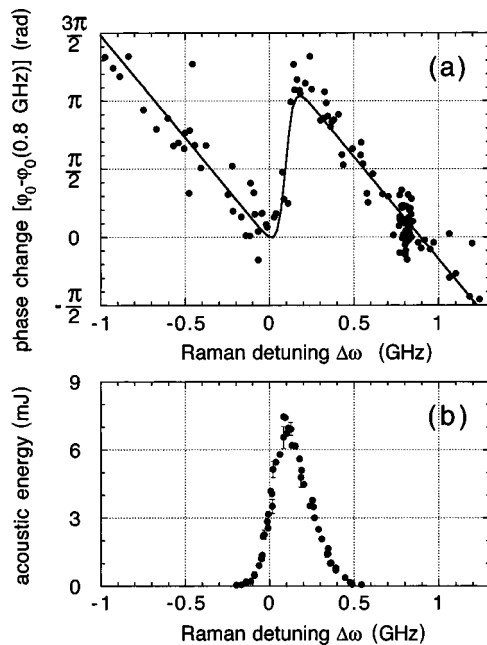
FIG. 3. (a) Molecular phase spectroscopy: relative shift of the fringe pattern of Fig. 2 vs Raman detuning. The solid line shows a linear dispersion slope and a π-radian phase step-up on resonance. (b) Acoustic Raman spectroscopy: acoustic signal, which is proportional to the resonant nonadiabatic molecular excitation, as a function of Raman detuning.

We further ascertain the position of line center by putting a commercial dynamic audio microphone into the D_2 cell and measuring the amplitude of the shock wave produced by the laser energy that is absorbed in the medium. Figure 3(b) shows the acoustic signal as a function of the Raman detun-

ing. We attempt an absolute calibration of the microphone by measuring a sound wave produced by an 8-mJ, 1.06-μm laser pulse hitting black laser-burn paper inside the D_2 cell. We find, perhaps fortuitously, that the measured energy, required to produce the shock wave (7 mJ), is within a factor of 2 of the total laser energy, absorbed through the resonant Raman process (12 mJ).

In summary, this paper demonstrates the ability to independently adjust the phases of three sidebands, which are obtained from the collinear Raman generator and spaced by the molecular vibrational frequency, so as to produce amplitude or frequency modulated light. The AM component is detected due to its ability to excite molecular oscillations. We use our AM-detection technique to measure the relative phase among Raman sidebands, as a function of the Raman detuning.

By adjusting the phases of additional sidebands, either manually, or by spectral modification techniques [5], one should be able to synthesize a periodic train of arbitrarily shaped pulses [6,7]. While a single-pulse selection is theoretically possible, there are a number of experiments in which a train of pulses can be preferred. These experiments include multiphoton ionization studies with about four octaves of bandwidth, coherent atomic and molecular control, and the synthesis of unique sets of phased frequencies that may propagate through the medium without change. These eigenvectors may be of the self-induced transparency type as suggested by Kaplan [8], or the electromagnetically induced transparency type as suggested by Yavuz *et al.* [9].

[1] A. V. Sokolov, D. R. Walker, D. D. Yavuz, G. Y. Yin, and S. E. Harris, Phys. Rev. Lett. **85**, 562 (2000).

[2] In a similar experiment, Liang *et al.* demonstrated efficient replication of broadband signal into a different spectral region: J. Q. Liang, M. Katsuragawa, Fam Le Kien, and K. Hakuta, Phys. Rev. Lett. **85**, 2474 (2000).

[3] Y. R. Shen, *The Principles of Nonlinear Optics* (J. Wiley, New York, 1984).

[4] S. E. Harris and A. V. Sokolov, Phys. Rev. A **55**, R4019 (1997); Phys. Rev. Lett. **81**, 2894 (1998); A. V. Sokolov, D. D. Yavuz, and S. E. Harris, Opt. Lett. **24**, 557 (1999); A. V. Sokolov, *ibid.* **24**, 1248 (1999).

[5] C. W. Hillegas, J. X. Tull, D. Goswami, D. Strickland, and W. S. Warren, Opt. Lett. **19**, 737 (1994); A. M. Weiner, Prog.

Quantum Electron. **19**, 161 (1995); T. Baumert, T. Brixner, V. Seyfried, M. Strehle, and G. Gerber, Appl. Phys. B: Lasers Opt. **65**, 779 (1997).

[6] Hansch has previously proposed a pulse synthesizer that uses separate phase-locked laser oscillators: T. W. Hansch, Opt. Commun. **80**, 71 (1990).

[7] The phase of the carrier frequency, with respect to the phase of the modulation envelope, can be fixed if the ratio of the carrier frequency to the modulation frequency is an integer.

[8] A. E. Kaplan, Phys. Rev. Lett. **73**, 1243 (1994); A. E. Kaplan and P. L. Shkolnikov, J. Opt. Soc. Am. B **13**, 347 (1996).

[9] D. D. Yavuz, A. V. Sokolov, and S. E. Harris, Phys. Rev. Lett. **84**, 75 (2000).